

# Theoretical Study of Bonding of Carbon Trioxide and Carbonate on Pt(111): Relevance to the Interpretation of “in Situ” Vibrational Spectroscopy

A. Markovits,<sup>†,‡</sup> M. García-Hernández,<sup>†</sup> J. M. Ricart,<sup>‡</sup> and F. Illas<sup>\*,†</sup>

*Departament de Química Física, Universitat de Barcelona, C/Martí i Franqués 1, 08028 Barcelona, Spain, and Departament de Química Física i Inorgànica, Universitat Rovira i Virgili, Pl. Imperial Tàrraco 1, 43005 Tarragona, Spain*

*Received: October 8, 1998*

The interaction of carbon trioxide and carbonate on Pt(111) has been studied through the ab initio cluster model approach within the Hartree–Fock and hybrid density functional theory based methods. The equilibrium geometry of adsorbed CO<sub>3</sub> and CO<sub>3</sub><sup>2−</sup> are found to be very similar, suggesting that, once on the surface, both molecules lead to the same adsorbed species but having different adsorption energies. This behavior is rationalized in terms of cost–benefit arguments. The analysis of the vibrational frequencies leads to several important conclusions. The most important one is that vibrational frequencies of the adsorbed species are not always comparable to those of carbonate complexes. However, it is shown that the vibrational frequency for the highest A<sub>1</sub> normal internal mode can be transferred from the complex to the surface. The theoretical analysis is next used to interpret the “in situ” infrared spectra of adsorbed carbonate in an electrochemical environment.

## I. Introduction

The specific adsorption of anions on the surface of electrodes has long been known to play a crucial role in electrochemistry.<sup>1</sup> However, very little is known about the microscopic mechanisms by which these adsorbed anions can modify the reactions that take place at the electrode surface. This limited knowledge arises from the very complex structure of the electrochemical double layer, where there is a delicate interplay between different physical phenomena such as electric fields, solvent effects, adsorption, coadsorption, and surface structure.<sup>2</sup> The microscopic study of this important phenomenon has been possible thanks to the application of surface science techniques to electrochemistry. Hence, a rather simple technique to prepare single-crystal electrodes was first introduced by Clavilier,<sup>3,4</sup> and “in situ” spectroscopic techniques have also been developed.<sup>5</sup> These “in situ” techniques are aimed to give information about the adsorption site and interaction mode. Here, we must stress the fact that assignment of the adsorption sites based only on vibrational data is in general not unique and has to be regarded with extreme caution. For instance, quantitative surface structure analysis based on photoelectron diffraction techniques<sup>6,7</sup> has unambiguously shown that NO on Ni(111) is chemisorbed in the 3-fold open site despite exhibiting a vibrational shift that would suggest a bridge site.

In the case of electrochemistry, vibrational spectroscopy is one of the few experimental techniques that allows one to obtain microscopic information about the structure and bonding modes of adsorbed ions. This is because of the difficulty to transfer other quantitative surface structure analysis techniques, often requiring ultrahigh vacuum conditions, to the electrochemical environment. Therefore, a large amount of work has been devoted to obtaining and interpreting “in situ” infrared spectra for oxyanions in electrochemical interfaces.<sup>8–12</sup> Moreover, one

needs to consider the fact that the adsorption mode of an adsorbate usually depends on the surface structure.<sup>9,10</sup> Hence, in the addition of “in situ” techniques, the electrodes must exhibit well-defined surfaces.<sup>11</sup> However, even in these sophisticated electrochemical experiments, the interpretation of the spectra is far from being straightforward and comparison to existing well-known molecular species or complexes is unavoidable. Hence, a feature that is exploited by experimentalists is that, during the adsorption process, the adsorbate often lowers its symmetry, and one can exploit the correlation between the normal modes of the free and adsorbed species to assign a particular mode or a surface site. Let us take the carbonate anion as an example. The free CO<sub>3</sub><sup>2−</sup> molecule in the gas phase has a rather high symmetry; it belongs to the D<sub>3h</sub> point group, with the three oxygen atoms being equivalent. Because of this high symmetry, some normal vibrational modes are degenerated. However, once the carbonate is adsorbed, only two oxygen atoms are equivalent. Thus, the adsorbed molecule lowers its symmetry to that of the C<sub>2v</sub> group. The important point is that this symmetry lowering causes a splitting of the gas-phase molecule degenerated modes. Yet, this splitting depends on the strength of the adsorption bond and on the adsorption, or coordination, modes. In fact, by considering the magnitude of the splitting, the spectroscopists can have precise information on the coordination mode at the molecular level.<sup>13,14</sup> While this approach permits one to distinguish monodentate and bidentate carbonate complexes,<sup>15</sup> it is not clear that a direct comparison to the case of carbonate adsorption on metal surfaces would give an univocal answer. This is because, on one hand, there are situations that appear on the surface and are not present in carbonate complexes (i.e., consider the case of a monodentate coordination above a 3-fold site) and, on the other hand, one must not forget that a given ligand bonded to a surface exhibits a different chemical bond than that in a molecular complex.

The adsorption of carbonate species on single-crystal platinum electrodes has been precisely the object of a number of

<sup>†</sup> Universitat de Barcelona.

<sup>‡</sup> Universitat Rovira i Virgili.

experimental studies. These include "in situ" IR measurements of the vibrational frequencies of carbonate adsorbed on Pt(111) and Pt(110) single-crystal electrodes.<sup>12,16–19</sup> Again, the interpretation of the measured IR bands is based on the comparison to existing carbonate complexes. The lack of quantitative surface science experiments about coordination modes and surface sites, adsorption geometries, and vibrational frequencies for a similar system does not permit a definitive and univocal assignment of the IR bands, nor does it permit a picture of the bonding mechanism of carbonate anions to a Pt surface. A way to circumvent these difficulties is to make use of theoretical models that permit the answers to the above-described questions to be obtained. This is indeed the aim of the present work. Hence, the *ab initio* cluster model approach<sup>20–27</sup> will be applied to the study of carbonate and CO<sub>3</sub> on Pt(111). This theoretical approach permits a detailed analysis of the surface chemical bond and, depending on the quality of the *ab initio* wave function, a rather quantitative description of several properties.

To the best of our knowledge, the results reported by Iwasita et al.<sup>12</sup> constitute the only IR studies concerning the adsorption of carbonate on Pt(111). We will take this work as the experimental reference for the present theoretical study aimed to provide information about the bonding mechanism and structural data for carbonate of Pt(111). We will refer to the Iwasita work<sup>12</sup> even if the present theoretical study does only contain a few results involving electric field or solvent effects. We will present evidence supporting the reasonable assumption that the electric field effects are second order with respect to the coordination mode and surface site. In addition, we will show that solvation effects are likely to induce small shifts on the vibrational frequencies without changing the qualitative description.

This work is organized as follows. Section II describes the surface cluster models employed and the several coordination modes considered. The theoretical approaches and computational details are described in section III. Next, in section IV, we describe the equilibrium structural parameters obtained for adsorbed carbonate and also for the neutral CO<sub>3</sub> species. The bonding mechanism and adsorption energies for the different coordination modes of carbonate and CO<sub>3</sub> are given in section V, whereas the discussion concerning vibrational frequencies for adsorbed carbonate is reported in section VI. Finally, in section VII, we present our conclusions.

## II. Surface Cluster Models

The Pt(111) surface has been modeled by means of reasonably large cluster models. Different clusters are used to represent different coordination modes and different surface sites, although in some cases, the same cluster is used to study chemisorption on different sites. This strategy permits the delimiting of the influence of the cluster models on the calculated properties. As usual, the clusters are denoted as Pt<sub>*n*</sub>(*k,l,m*) where *n* stands for the total number of atoms in the cluster and (*k,l,m*) describe the number of atoms in the first, second and third layers. The clusters models that we have used are schematically represented in Figure 1 and can be designated as Pt<sub>13</sub>(7,3,3), Pt<sub>18</sub>(12,6), and Pt<sub>20</sub>(10,5,5). The two first clusters have C<sub>3v</sub> symmetry, whereas the third one belongs to the C<sub>s</sub> symmetry group. In any case, the presence of the adsorbates lowers the symmetry, and in most of the cases, the cluster plus adsorbate supersystem does not present any symmetry.

To avoid any possible bias or cluster artifacts arising from the use of a charged adsorbate such as the carbonate anion, we have also considered the adsorption of the neutral CO<sub>3</sub> species.

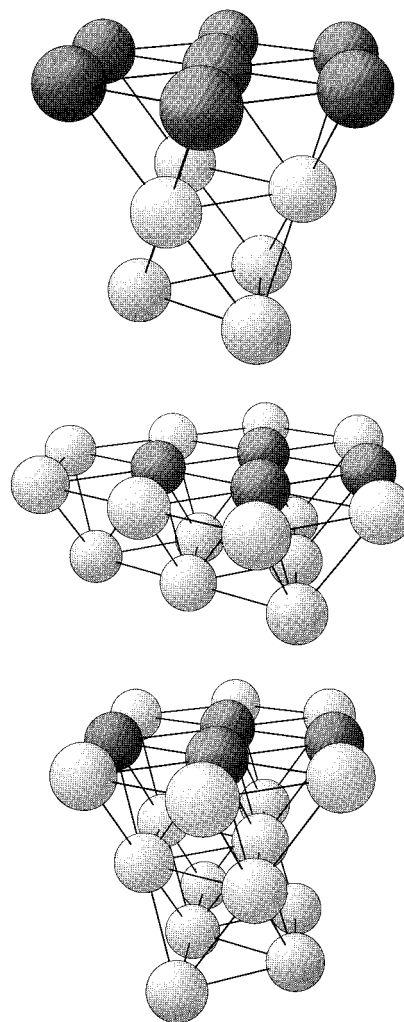


**Figure 1.** Cluster models used to simulate different sites of the Pt(111) surface: (a) Pt<sub>13</sub>(7,3,3); (b) Pt<sub>18</sub>(12,6); (c) Pt<sub>20</sub>(10,5,5). The darker atoms correspond to the "local" region, whereas the light ones define the "outer" region (see section III).

In the real experiment, there is only one adsorbed species, but because of the complexity of the conditions on which electrochemical experiments are carried out, it is very difficult to identify the nature of the adsorbate. The comparison of the final geometries for both adsorbed species is a theoretical stratagem that permits us to show that a unique adsorbed species is found regardless of the one used in the model calculation. This is in agreement with the preliminary results of Paredes et al. who considered carbonate and CO<sub>3</sub> on silver surfaces.<sup>28</sup> The appearance of the IR bands in the experiments carried out by Iwasita et al.<sup>12</sup> means that the adsorbed carbonate is oriented with the molecular plane perpendicular to the surface. For a flat orientation parallel to the surface, vibrational excitations concerning the internal carbonate modes are forbidden and are not present in the IR spectra.<sup>5</sup> Accordingly, only situations where the CO<sub>3</sub> or carbonate plane are perpendicular to the surface have been considered. These perpendicular orientations can be classified as monodentate, MD, or bidentate, BD, depending on whether one or two oxygen atoms directly interact with the surface. For the MD coordination mode, three different possibilities have been explicitly considered (Figure 2); these are the ones where an oxygen atom of the adsorbed species is directly above a surface Pt atom, atop-MD, or above one of the two, fcc or open and hcp or eclipsed, 3-fold sites, fcc-MD and hcp-MD, respectively. Similarly, two coordinations modes have

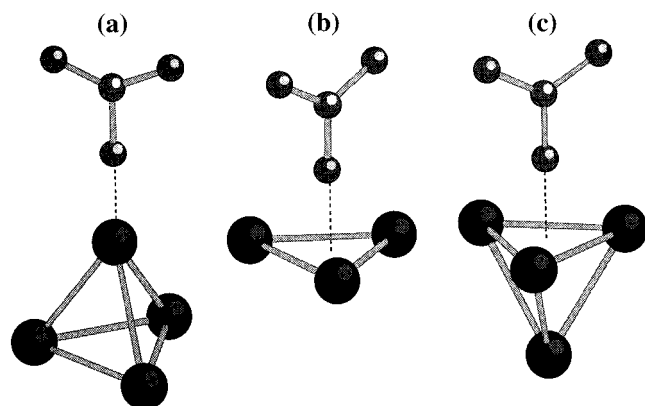


**Figure 2.** Three different monodentate coordination modes considered in the present work: (a) on top above a Pt atom, atop-MD; (b) above an fcc open hollow site, fcc-MD; (c) above an hcp, eclipsed hollow site, hcp-MD.

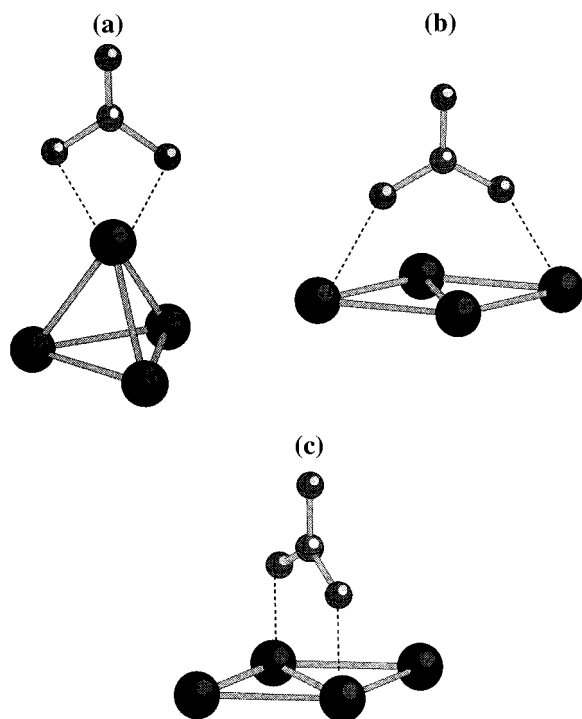


**Figure 3.** Three bidentate coordination modes: (a) chelating bidentate, ch-BD; (b) long bridge, lg-BD; (c) short bridge, sh-BD.

been considered for the BD case, depending on whether the two oxygen atoms directed toward the surface interact with one or two surface Pt atoms. In the first case, we have a chelating coordination mode, hereafter named ch-BD, whereas two possibilities appear for the BD case, depending on whether the two oxygen atoms are directed toward two opposite Pt atoms across a short-, sh-BD, or long-bridge, lg-BD, “bond” of the Pt(111) surface (Figure 3). For the atop-MD case, the Pt<sub>13</sub> cluster has been chosen, whereas Pt<sub>20</sub> has been used to study both fcc-MD and hcp-MD modes. For the BD cases, Pt<sub>13</sub> has been selected to represent the ch-BD mode, and both Pt<sub>18</sub> and Pt<sub>20</sub> have been considered for the sh-BD and lg-BD coordination modes. Finally, we would like to comment that smaller clusters have also been used to identify the normal models of adsorbed carbonate. These smaller clusters are suitable reductions of the ones described above.

Before closing this section, we would like to point out that the largest clusters used in this work, Pt<sub>18</sub> and Pt<sub>20</sub>, may be too small to represent some properties of the extended surface. For

instance, these clusters do not permit it to reach convergence on the calculated binding energy.<sup>29–31</sup> This is a limitation of the cluster model approach that is especially astringent when the conclusions are mainly based on the binding energy. However, the main goal of the present paper is to interpret the IR spectra of adsorbed carbonate. The vibrational frequencies corresponding to the carbonate internal modes are a local property. We will present evidence that this is indeed the case.

### III. Computational Details

The electronic structure of the Pt<sub>13</sub>, Pt<sub>18</sub>, and Pt<sub>20</sub> cluster models interacting with the CO<sub>3</sub> and carbonate species on the different coordination modes has been investigated starting from the well-known *ab initio* Hartree–Fock method (HF), and electronic correlation effects were included through the recently proposed and widely used B3LYP hybrid, nonlocal, density functional theory (DFT) method.<sup>32</sup> We must stress the fact that the hybrid B3LYP approach was initially designed to reproduce thermochemical data on a series of mainly organic molecules. However, recent studies have shown that this hybrid approach performs reasonably well for transition-metal-containing systems<sup>33–35</sup> including metal–oxide and adsorbate–metal interaction<sup>36,37</sup> and is able even to reproduce, although in a qualitative way, the trends of magnetic coupling in both ionic solids<sup>38</sup> and binuclear complexes.<sup>39</sup>

In either method, HF or B3LYP, the molecular orbitals have been expressed as a linear combination of Gaussian-type orbitals. A standard split valence plus polarization basis set, 6-31G\*, has been employed to describe the C and O atoms on the carbonate and CO<sub>3</sub> species. Diffuse functions usually necessary to achieve a reasonable description of isolated anions were not included here because the 6-31G\* description of free carbonate either at the HF or B3LYP levels is accurate enough for the present purposes; the error in the C–O distance is less than 0.02 Å, and the calculated B3LYP frequencies have an error of about 3% with respect to experimental values. A mixed approach was used to describe the surface cluster models. In this approach, the cluster was divided into a “local” and an “outer” region. The “local” region contains the atoms that are directly involved with the adsorbate, whereas the “outer” region is mainly devoted to provide an adequate environment to the “local” one and to improve the representation of the metal conduction band. For the Pt<sub>13</sub> cluster, the seven atoms on the first layer are included in the “local” region, although we have also explored the case where only the first layer center atom is included in the “local” region. For Pt<sub>18</sub> and Pt<sub>20</sub>, the “local” region is defined by the four cluster atoms wrapping the bridge site. For the atoms on the “local” site, we replaced the inner core electrons by the relativistic, small core effective core potentials, RECP, reported by Hay and Wadt and explicitly included the 5s<sup>2</sup>5p<sup>6</sup>5d<sup>10</sup> electrons, which are described by their standard double- $\zeta$  basis set.<sup>40</sup> For the Pt atoms in the “outer” region, we used a recently developed one-electron pseudopotential,<sup>41,42</sup> which is appropriated to be used for embedding purposes.<sup>43–46</sup> This one-electron pseudopotential was initially derived in the form of Durand and Barthelat<sup>47</sup> and later fitted to the Hay and Wadt form<sup>40</sup> to allow its use in most of the available computer codes. The basis set for the one-electron Pt pseudoatoms was chosen as [5s3p/2s1p].

For each one of the coordination modes and adsorption sites described in the previous section, the internal geometry of the adsorbed molecule, CO<sub>3</sub> and CO<sub>3</sub><sup>2–</sup>, and the distance to the surface were optimized with the only restriction being keeping the C<sub>2v</sub> symmetry of the adsorbed molecule. Since the calculations are carried out self-consistently for the adsorbate plus surface



**TABLE 1: Equilibrium Geometrical Parameters for the Monodentate, MD, Adsorption of  $\text{CO}_3$  and  $\text{CO}_3^{2-}$  in the atop, fcc, and hcp Surface Sites<sup>a</sup>**

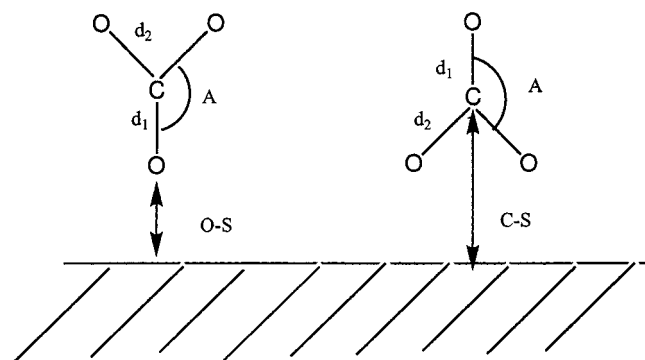
adsorption mode	cluster mode	comput method	$\text{CO}_3$				$\text{CO}_3^{2-}$			
			O-S	$d_1$	$d_2$	A	O-S	$d_1$	$d_2$	A
atop-MD	Pt <sub>13</sub>	HF	1.950	1.410	1.222	113.7	1.996	1.347	1.244	116.8
		B3LYP	2.224	1.298	1.253	117.6	2.365	1.304	1.264	118.4
fcc-MD	Pt <sub>20</sub>	HF	Dissociates into $\text{CO}_2 + \text{O}$ (ads)				1.602	1.394	1.231	115.1
		B3LYP	1.598	1.459	1.231	111.8	1.634	1.461	1.242	113.4
hcp-MD	Pt <sub>20</sub>	HF	Dissociates into $\text{CO}_2 + \text{O}$ (ads)				1.608	1.389	1.232	115.3
		B3LYP	Dissociates into $\text{CO}_2 + \text{O}$ (ads)				1.706	1.449	1.243	113.7

<sup>a</sup> O-S stands for the perpendicular distance between the surface site and the oxygen atom pointing toward the surface,  $d_1$  and  $d_2$  are the CO distances for the unequivalent, surface-coordinated oxygen and the two equivalent oxygen atoms, respectively, and A stands for the O-C-O angle involving unequivalent oxygen atoms.

**TABLE 2: Equilibrium Geometrical Parameters for the Bidentate, BD, Adsorption of  $\text{CO}_3$  and  $\text{CO}_3^{2-}$  on the Chelating, Short-Bridge, and Long-Bridge Coordination Modes<sup>a</sup>**

adsorption mode	cluster mode	comput method	$\text{CO}_3$				$\text{CO}_3^{2-}$			
			C-S	$d_1$	$d_2$	A	C-S	$d_1$	$d_2$	A
ch-BD	Pt <sub>13</sub>	HF	2.563	1.186	1.317	125.4	2.641	1.212	1.303	123.8
		B3LYP	2.717	1.220	1.312	124.0	2.916	1.254	1.300	120.1
sh-BD	Pt <sub>18</sub>	HF	2.630	1.202	1.310	119.0	2.624	1.214	1.304	120.0
		B3LYP	2.683	1.226	1.330	121.7	2.697	1.237	1.325	122.3
	Pt <sub>20</sub>	HF	2.607	1.197	1.314	120.4	2.684	1.220	1.301	119.4
		B3LYP	2.694	1.231	1.317	124.2	2.782	1.246	1.324	121.4
lg-BD	Pt <sub>18</sub>	HF	2.571	1.202	1.319	115.4	2.584	1.216	1.313	117.6
		B3LYP	2.615	1.223	1.344	119.8	2.619	1.241	1.331	122.0
	Pt <sub>20</sub>	HF	2.554	1.201	1.322	117.7	2.836	1.233	1.302	116.7
		B3LYP	2.709	1.235	1.318	124.3	2.821	1.251	1.318	122.5

<sup>a</sup> C-S stands for the perpendicular distance between the surface site and the carbon atom,  $d_1$  and  $d_2$  are the CO distances for the unequivalent oxygen and the two equivalent, surface-coordinated oxygen atoms, respectively, and A stands for the O-C-O angle involving unequivalent oxygen atoms.

**Figure 4.** Geometrical parameters defining the geometry of adsorbed carbonate; see Tables 1 and 2.

model, the surface electric dipole, its interaction with the adsorbate, and the surface response are explicitly accounted for although in a qualitative way because of the cluster limitations described above. Analytical gradients were always used to search for the optimum geometrical parameters. Vibrational frequencies were computed in a two-step procedure. First, a small cluster model was used to obtain the normal coordinates of an adsorbed species. This step was carried out by first optimizing the geometry of the molecule above the reduced cluster model (vide infra) and then computing the vibrational frequencies by explicit diagonalization of the Hessian matrix and considering infinite substrate mass to decouple the internal modes from the surface phonons. In the second step, once the normal modes are determined, the vibrational frequency of a given mode can be easily calculated for the molecule interacting with the larger cluster models. This procedure permits a reasonable estimate of the vibrational frequencies of the adsorbed molecule to be obtained without needing to construct the Hessian matrix for the large cluster, resulting in a substantial saving of computer time.

To better simulate the conditions on which IR “in situ” electrochemical experiments are carried out, some frequency calculations have been carried out in the presence of an external uniform electric field.<sup>48,49</sup> This theoretical procedure is commonly used to mimic the conditions of an electrochemical experiment. While this approach does not permit a one-to-one correspondence with the potential at which the experiment is actually carried out, it permits the addition of the main physical effect and investigation of its influence on the vibrational frequencies of the adsorbates.

All calculations were carried out using the Gaussian 94 suite of programs<sup>50</sup>

#### IV. Equilibrium Structural Parameters

To minimize possible cluster artifacts arising from the difficulty to equally describe charge-transfer effects from or toward the surface, two different adsorbates only differing in their total charge have been considered. These adsorbates are carbon trioxide, a neutral molecule, and the carbonate anion. The optimized HF and B3LYP geometric parameters of carbon trioxide and carbonate are given in Table 1 and Table 2 for the monodentate, MD, and bidentate, BD, coordination modes, with the relevant geometrical parameters being schematically depicted in Figure 4. We recall that, in the gas phase,  $\text{CO}_3$  and  $\text{CO}_3^{2-}$  belong to the  $C_{2v}$  and  $D_{3h}$  symmetry groups, respectively, and the electronic ground state of both molecules is a singlet resulting from a closed shell occupancy. The adsorbate has always a  $C_{2v}$  symmetry, independently of the adsorption mode. In the case of the monodentate adsorption mode, one oxygen interacts with the surface while the two others are oriented against it. In the case of the bidentate adsorption modes, there are two oxygen atoms directly linked to the surface. We must stress the fact that in all MD cases and on the ch-BD one the

rotation of the adsorbed molecule around the  $C_2$  axis is almost free.

An important result of the present model calculations is that, once bonded to the surface, the resulting adsorbed species has almost the same geometry, independently of its initial charge, coordination mode, and surface site. This is an expected result for an adsorbate in a metal surface; the metal being a conductor can delocalize the extra charge on the bulk. In fact, previous studies for sulfur oxides on gold and silver surfaces have also found that the geometry of the adsorbed polyatomic anion is independent of the charge and presented a thermodynamic argument that shows that this should be the case in the low coverage limit.<sup>29,30</sup> The fact that the calculated geometry does not depend on the initial charge is a clear indication that the present clusters do adequately represent the metal surface. On the other hand, the small differences in the geometries of adsorbed carbon trioxide or adsorbed carbonate plus the difference in the perpendicular distance of the adsorbate to the surface indicate that the representation of the metal surface is not perfect. The geometry of the adsorbed molecules is only slightly different in the case of the monodentate adsorption at the HF level, although the difference is not present in the B3LYP results.

For all MD modes, the C–O distance for the unequivalent oxygen atom,  $d_1$  in Figure 4, is noticeably larger than that for the BD cases;  $d_1$  is  $\sim 1.30$ – $1.40$  Å for the MD modes, while it is in the  $1.18$ – $1.26$  Å range for the BD coordination modes. The explanation is fairly simple if one considers the coordination of the oxygen atoms. In the MD adsorption, one oxygen atom interacts with one Pt surface atom and with the carbon atom. Therefore, the interaction with the surface diminishes the strength of the C–O, surface-coordinated bond. This leads to  $d_1$  values which are bigger in the MD case. As a consequence of the diminution of the C–O, surface-coordinated bond strength, the C–O, noncoordinated bond strength increases and its bond length decreases. In the case of the BD adsorptions, the mechanism is just reversed and  $d_1$  is shortened with respect to  $d_2$ .

Finally, it is worth pointing out that as far as the optimum geometries are concerned, the only noticeable effects arising from electronic correlation, HF versus B3LYP results, are on the adsorbate–surface distance. This is hardly surprising since it is well-known that the accurate description of the adsorbate–metal surface bond requires explicit inclusion of electronic correlation.<sup>23–27</sup>

## V. Bonding Mechanism and Adsorption Energies

The discussion in the previous section strongly suggests that, once on the surface, carbon trioxide and carbonate become the same adsorbed species. This is found to be the case for both the HF and B3LYP levels of calculation. This adsorbed species must then have a given net charge that will not depend on the initial species. The precise measure of this net charge is not a simple question, although qualitative information can be found through the Mulliken population analysis. We must caution that the Mulliken charges cannot be taken as absolute measures of atomic charges. In some cases, the prediction from Mulliken is totally erroneous; i.e., an ionic system such as bulk NiO is predicted to be covalent!<sup>51</sup> The present use of Mulliken charges is completely qualitative, and the aim is to compare similar systems within the same basis set and compare HF to B3LYP descriptions. To avoid the reader getting lost in an ocean of numbers, we have deliberately omitted a lengthy listing of the calculated net charges. Instead, we will just carry out the

discussion based on the general trends. For a given coordination mode in a given site, the net charge on  $\text{CO}_3$  and  $\text{CO}_3^{2-}$  is qualitatively the same for both HF and B3LYP methods, although B3LYP net charges are systematically smaller than the HF values. The HF wave function predicts a net charge on the adsorbed species of about  $-1.2 \pm 0.2$  electrons, whereas the B3LYP value is significantly smaller, ranging from  $-0.9$  to  $-0.3$  electrons, depending on the adsorption site. The different description of the net charge of the adsorbed species resulting from both methods is in agreement with the general belief that HF overestimates the ionicity. However, this statement cannot be proven without further theoretical analysis. Below, we will show that the origin of this significant difference is precisely related to the different energetic description of the charge-transfer process at the HF and B3LYP levels.

To understand the bonding mechanism and the Mulliken populations described above, let us assume that a reasonable estimate of the final net charge on the adsorbed species is about  $-1$  e. This means that  $\text{CO}_3$  will take one electron from the cluster model whereas  $\text{CO}_3^{2-}$  will give one electron to the surface. In the real Pt(111) metal surface, the first process will cost 5.7 eV, i.e., the Pt(111) work function. However, the second process will release exactly the same amount of energy. Since the electron affinity of carbon trioxide is much smaller and the covalent bond contribution will be the same for both cases,  $\text{CO}_3$  and  $\text{CO}_3^{2-}$ , it is easy to predict that the adsorption energy of  $\text{CO}_3^{2-}$  will be much larger. Later, we will show that this is definitely the case. The present interpretation of the bonding mechanism also permits explanation of the HF larger value of the adsorbed species net charge as compared to the B3LYP values. We have just commented on the fact that for a real metal surface the energy necessary to ionize one electron from the surface is exactly the same as the energy gained when one electron is added to it. Also, it is known that the HF method provides reasonable estimates of the ionization potential, IP, of a given system but in most cases cannot even qualitatively predict the existence of negative anions. On the other hand, the B3LYP methods takes into account, perhaps not in an exact way, the electronic correlation effects and permits a better description of these systems. Hence, the larger negative net charge on the adsorbate found by the HF description reflects the difficulty of this method in describing the metal cluster electron affinity, EA. The B3LYP description is no doubt better and the charges derived from the B3LYP density should be more precise. However, the cluster's IP and EA B3LYP values are not still the same; the cluster IP for  $\text{Pt}_{13}$  is 6.00 eV, close to the Pt(111) work function, but the cluster EA is of only 2.3 eV. The fact that the EA of the cluster is too small as compared to the cluster IP cannot be avoided by using a more exact quantum chemical method. It represents a limitation of the cluster model approach. This limitation has been previously recognized by Pacchioni and Bagus<sup>52,53</sup> in their study of K on Cu(100). Because of this limitation, in the present case, it is not possible to obtain accurate values of the interaction energy when one electron is transferred to the surface. Nevertheless, this limitation does not invalidate the cluster model description, it just establishes limits for the prediction of the interaction energies.

The following discussion concerning calculated adsorption energies is based on the B3LYP results. In view of the preceding discussion, the adsorption energies for  $\text{CO}_3$  are probably more accurate than those for  $\text{CO}_3^{2-}$ , which will be underestimated because of the error in the cluster EA. Nevertheless, the purpose of the present work is not to obtain accurate values for the adsorption energies but to rationalize the binding mechanism,

**TABLE 3: Calculated, B3LYP, Adsorption Energies (kcal/mol) for CO<sub>3</sub> and CO<sub>3</sub><sup>2-</sup> in the Monodentate, MD, Adsorption Mode on the atop, fcc, and hcp Surface Sites and for the Bidentate, BD, Adsorption Mode on the Chelating, Short-Bridge, and Long-Bridge Coordination Modes**

adsorption mode	cluster model	CO <sub>3</sub>	CO <sub>3</sub> <sup>2-</sup>
atop-MD	Pt <sub>13</sub>	4.5	127.0
fcc-MD	Pt <sub>20</sub>	26.5	128.7
hcp-MD	Pt <sub>20</sub>		122.0
ch-BD	Pt <sub>13</sub>	20.7	131.9
sh-BD	Pt <sub>18</sub>	67.5	155.4
	Pt <sub>20</sub>	56.7	150.5
lg-BD	Pt <sub>18</sub>	31.3	100.6
	Pt <sub>20</sub>	28.5	127.2

compare CO<sub>3</sub> to CO<sub>3</sub><sup>2-</sup>, and compare the adsorption on different sites. The B3LYP adsorption energies for CO<sub>3</sub> to CO<sub>3</sub><sup>2-</sup> are given in Table 3. As usual, these values have been calculated as the negative difference between the energy of the Pt<sub>n</sub> cluster plus the adsorbate at the optimum geometry minus the energy of the separated units, with positive values meaning a favorable interaction.

The calculated adsorption energies for CO<sub>3</sub> and CO<sub>3</sub><sup>2-</sup> are in agreement with the bonding mechanism described above. The values for carbon trioxide are much smaller than those for the carbonate. Moreover, the relatively large values found for the carbonate adsorption energy are in agreement with the experimental findings of Iwasita.<sup>12</sup> These authors have studied the adsorption of carbonate on Pt(111) single-crystal electrodes. They have obtained a voltammogram using a well-ordered, single-crystal Pt(111) electrode with and without carbon dioxide in a 0.1 M HClO<sub>4</sub> solution. Their results are typical of an anion adsorption. The Pt oxide formation observed at 1.05 V is inhibited in the presence of CO<sub>2</sub> in the 0.1 HClO<sub>4</sub> solution. Iwasita et al.<sup>12</sup> concluded that a relatively strong adsorption of the anion exists. A particularly interesting result derived from the present calculations is that the relative order of stabilities for CO<sub>3</sub> and CO<sub>3</sub><sup>2-</sup> is the same; the most favorable situation appears to be the short-bridge bidentate coordination mode. Another intriguing feature is the dependency of the adsorption energies with respect to the cluster size. For the CO<sub>3</sub><sup>2-</sup> sh-BD mode, the adsorption energies arising from both Pt<sub>18</sub> and Pt<sub>20</sub> are very similar; they differ by ~5 kcal/mol only. However, for the lg-BD mode on the same clusters, the CO<sub>3</sub><sup>2-</sup> adsorption energies differ by ~27 kcal/mol! This difference correlates with the differences in the geometrical parameters found for the Pt<sub>18</sub> and Pt<sub>20</sub> clusters when the lg-BD case is considered. This result clearly shows how dangerous it is to rely on the absolute values of the calculated energies even when large cluster models and accurate quantum chemical model are used. We must stress the fact that only the adsorbate geometry was optimized and the adsorbate was always forced to stay above the active site chosen. Hence, it is well possible that some of the coordination modes studied do not represent real minima on the potential energy surface. The choice of different coordination modes is a convenient way to explore the potential energy surface and to obtain trends on several properties. In the next section, we will show that the vibrational frequencies for the short bridge are the most likely candidates to explain the observed experimental IR bands.<sup>12</sup> The use of the cluster model approach and the combined study of different properties permits identification of the limitations of the model itself, but also explanation of the chemical mechanisms involving complex phenomena and reasonable predictions concerning observable properties.

## VI. Vibrational Frequencies for Adsorbed Carbonate

First of all, we consider the vibrational frequencies of free carbonate and compare the B3LYP calculated values to the experimental figures reported by Herzberg.<sup>54</sup> The vibrational spectra of free carbonate exhibits four bands of E', A<sub>2</sub>'', A<sub>1</sub>', and E' symmetry appearing at 680, 879, 1063, and 1415 cm<sup>-1</sup>, respectively. The B3LYP calculated vibrational frequencies appear at 665, 876, 1014, and 1452 cm<sup>-1</sup>. Notice that these values are remarkably close to the experimental numbers, with the largest absolute deviation being 49 cm<sup>-1</sup> or 4%; the average error is less than 2%. The good agreement between calculated and experimental values for free carbonate should be transferable to the case of adsorbed carbonate. This point will be further reinforced by the comparison between experimental and calculated vibrational frequencies for the carbonate complex, which is used as a reference by Iwasita et al.<sup>12</sup> Consequently, we expect that the calculated values for adsorbed carbonate will be accurate enough so as to be used to interpret the "in situ" spectra reported in ref 12. As already pointed out, adsorption lowers the carbonate symmetry from D<sub>3h</sub> to C<sub>2v</sub> and splits the degenerated vibrational modes. This splitting is usually employed to discriminate between different adsorption modes.<sup>55</sup>

The vibrational frequencies of adsorbed carbonate have been first obtained by using cluster models with an explicit diagonalization of the Hessian matrix, i.e., within the harmonic approximation. For the atop-MD coordination mode, we have used Pt<sub>4</sub>(1,3), whereas Pt<sub>5</sub>(4,1) has been chosen to model the fcc-MD and hcp-MD coordination modes. The vibrational frequencies thus calculated have been found to be rather independent of the particular cluster model. In fact, for the hcp-MD, we have also used the Pt<sub>4</sub>(1,3), but the carbonate internal vibrational frequencies were almost unaffected. This result is hardly surprising and reflects the well-known fact that vibrational frequencies are characteristic of functional groups. For the BD coordination modes, the first estimate of the vibrational frequencies and normal coordinates has been carried out using Pt<sub>4</sub>(1,3) for the ch-BD and Pt<sub>4</sub>(4,0) for both sh-BD and lg-BD modes. To further verify the validity of the small cluster models and to check the accuracy of the vibrational frequencies obtained from those small models, we have carried out key calculations on the larger cluster models that have been used for the geometry optimization. Starting from the optimum geometry found using the large mode and for a given coordination mode in a given model, we have used the normal coordinates extracted from the small clusters and computed the energy potential curve along the normal coordinate. For the higher A<sub>1</sub> frequency and for the lg-BD adsorption mode, the values obtained through Pt<sub>20</sub> and Pt<sub>18</sub> are 1545 and 1592 cm<sup>-1</sup>, respectively. The small difference of ~45 cm<sup>-1</sup> provide a reasonable estimate of the uncertainty on the calculated frequencies. Notice that this is precisely the maximum error found for free carbonate. Thus, the error induced by the choice of one or another cluster is not larger than the intrinsic error of the present computational approach. On the other hand, the value predicted by the small Pt<sub>4</sub>, 1580 cm<sup>-1</sup>, is surprisingly close to the values calculated for the larger models, even if the optimum geometry of the adsorbed carbonate is not exactly the same for both clusters. For the same vibrational mode but for the sh-BD adsorption, we found 1657 cm<sup>-1</sup> on Pt<sub>18</sub> and 1679 cm<sup>-1</sup> on Pt<sub>4</sub>, whereas for the A<sub>1</sub> mode corresponding to the atop-MD, we obtain 1282 cm<sup>-1</sup> on Pt<sub>13</sub> and 1286 cm<sup>-1</sup> on Pt<sub>4</sub>(1,3).

The previous discussion concludes that the calculated frequencies for the small and large models are about the same. The comparison of the experimental and calculated values for

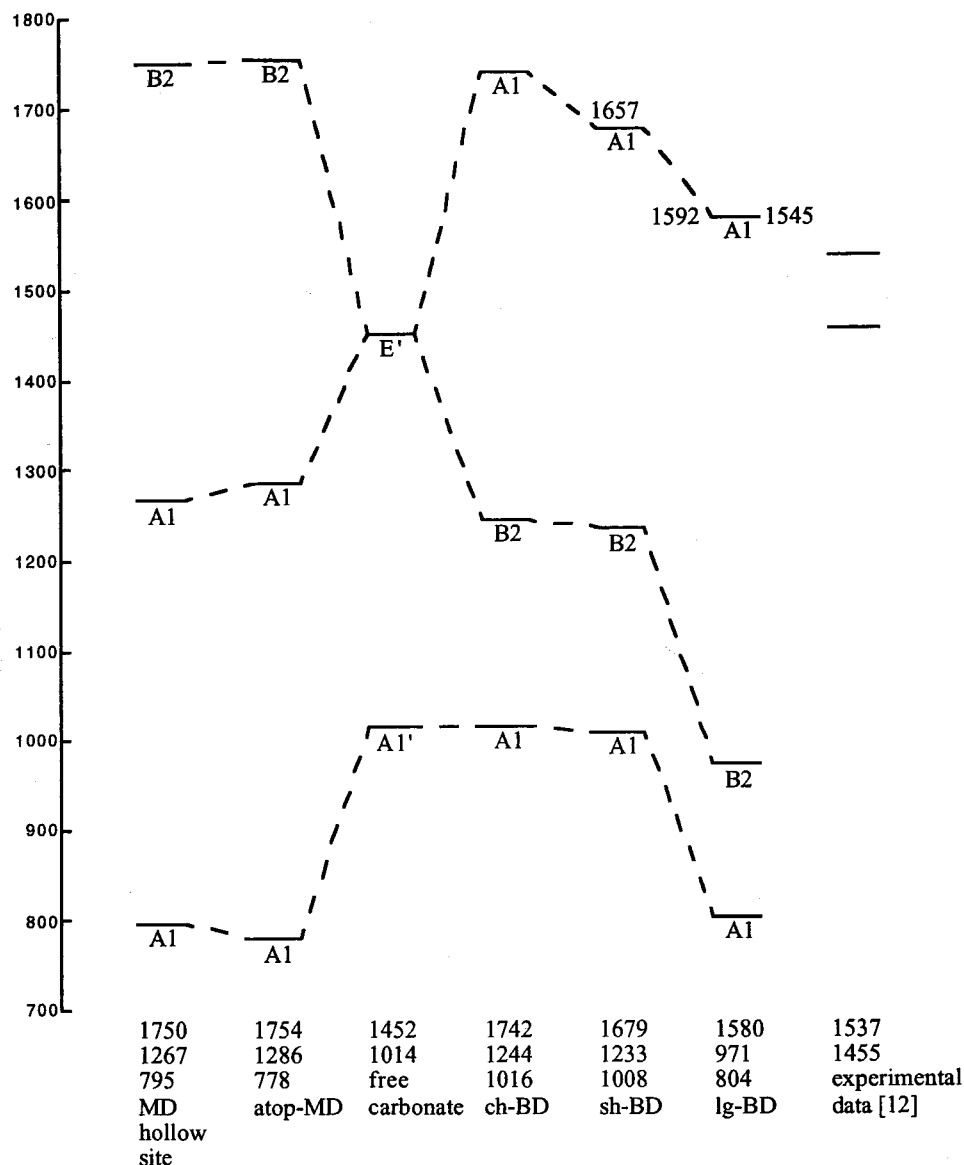


**Figure 5.** Calculated B3LYP vibrational frequencies obtained for the different adsorption modes of carbonate on the Pt cluster models. The values on the bottom correspond to those obtained for the smaller clusters, while those inside the figure have been obtained by means of the larger cluster models. The experimental results of Iwasita et al.<sup>12</sup> are also indicated.

the vibrational modes of free carbonate permits having reasonable confidence in the calculated values. Therefore, we will now use these calculated values to discuss the available experimental results concerning the vibrational modes of the carbonate. We will first describe the present results and then comment on those reported for carbonate complexes<sup>56,57</sup> and related species. The complete set of results is presented in Figure 5 where the calculated values are reported together to the variation of each vibrational frequency with coordination mode. For the MD, the three vibrational frequencies appear at 1750–1780  $\text{cm}^{-1}$  ( $B_2$ ), 1260–1290  $\text{cm}^{-1}$  ( $A_1$ ), and 780–785  $\text{cm}^{-1}$  ( $A_1$ ). For the BD cases, we found the well-known opposite splitting of the degenerate mode of free carbonate; for sh-BD and lg-BD, the frequencies are now at 1580–1680  $\text{cm}^{-1}$  ( $A_1$ ), 970–1230  $\text{cm}^{-1}$  ( $B_2$ ), and 800–1010  $\text{cm}^{-1}$  ( $A_1$ ). We have intentionally omitted the ch-BD in the description of the BD case above because the vibrational frequencies for ch-BD are almost identical to those of the MD case, except for the order of the two highest modes, which are of  $A_1$  and  $B_2$  symmetries contrary to the MD case where the order is  $B_2$  and  $A_1$ . The difference between the MD and BD is large enough to permit the assignment of the observed

frequencies to one or another coordination mode, except for the ch-BD that is indistinguishable from the MD cases. However, for a given coordination mode, when ch-BD is now considered as a “particular” case of MD coordination, the calculated frequencies are very close, thus precluding the use of vibrational information to distinguish among the different possibilities and adsorption sites, at least from the theoretical point of view.

Before comparing the frequencies obtained for the adsorbed carbonate to those reported for carbonate complexes, we find it convenient to discuss first the values reported in the literature. The vibrational spectra of Co(III) carbonate monodentate complexes were studied by two different groups many years ago.<sup>55–57</sup> Both groups report vibrational frequencies at 1450–1500  $\text{cm}^{-1}$  ( $B_2$ ), 1360–1380  $\text{cm}^{-1}$  ( $A_1$ ), and 1050–1070  $\text{cm}^{-1}$  ( $A_1$ ) that, in principle, are believed to arise from the carbonate internal modes. However, there is a disagreement concerning the assignment of these frequencies. Thus, Gatehouse et al.<sup>57</sup> state that the band at 1373  $\text{cm}^{-1}$  assigned to carbonate by Fujita et al.<sup>54,56</sup> is likely to be due to  $\text{NH}_3$  and  $\text{H}_2\text{O}$ , which absorb in the same region. Instead, Gatehouse et al. obtain a band at 1297



$\text{cm}^{-1}$  that is attributed to carbonate. However, for the so-called V4 band appearing at  $1453^{55,56}$  or  $1493\text{ cm}^{-1}$ <sup>57</sup> and for the one appearing at  $1050\text{ cm}^{-1}$ , both groups agree to assign them to carbonate. Since these values are quite different from the ones reported above for the different adsorbed species, we have decided to investigate the vibrational frequencies of the complex by using the same theoretical approach. Thus, the molecular structure of  $[\text{Co(III)}(\text{NH}_3)_5(\text{CO}_3)]^+$  has been optimized at the B3LYP level, which provides very good results for vibrational frequencies and related properties.<sup>31,58,59</sup> The B3LYP calculations for the complex used a small core RECP description for Co together with a double- $\zeta$  basis set and a 6-31G\* standard basis set for the rest of the atoms. Next, the optimized structure has been characterized as a true minimum and the vibrational frequencies have been calculated. Among the large set of vibrational frequencies for this complex we will discuss only those directly related to the present work; the complete study of the carbonate complex vibrational spectra will be reported elsewhere.<sup>60</sup> We obtain a frequency at  $1214\text{ cm}^{-1}$ , which is no doubt due to displacements related to the carbonate group; this is in agreement with the assignment of the band at  $1297\text{ cm}^{-1}$  by Gatehouse et al.<sup>57</sup> We also found a frequency at  $1440\text{ cm}^{-1}$ , very close to the experimental values of  $1453$  and  $1493\text{ cm}^{-1}$  reported in refs 55, 56, and 57, respectively. However, the analysis of the normal mode associated with this frequency reveals that it is not due to displacements in the carbonate group but to displacements on the  $\text{NH}_3$  ligands that are coupled to carbonate. Thus, this mode is related to carbonate but does not correspond to carbonate vibrations. Finally, we comment on the frequency appearing at  $1050\text{ cm}^{-1}$  in the experimental spectra. According to the present calculations, this is also a mode related to an  $\text{NH}_3$  ligands coupled to carbonate, with the calculated frequency being  $924\text{ cm}^{-1}$ . This brief comparison between calculated and experimental frequencies for the monocoordinated complex permits us to show that the calculated values can be trusted. Accordingly, we will not discuss theoretical calculations for the bidentate complex and will simply state that the main experimental modes for the highest frequencies appear at  $1590\text{--}1640\text{ cm}^{-1}$  ( $A_1$ ),  $1260\text{--}1290\text{ cm}^{-1}$  ( $B_2$ ), and  $1300\text{ cm}^{-1}$  ( $A_1$ ).<sup>14</sup>

Next, we can adequately compare the calculated frequencies for surface carbonate to those reported, or calculated, for carbonate complexes. For both MD plus ch-BD and BD cases, the calculated frequencies are far from those of the complex except for the highest  $A_1$  mode. In fact, the calculated  $B_2$  and lowest  $A_1$  for MD adsorbed carbonates are  $\sim 300\text{ cm}^{-1}$  different from the values in the monodentate complex. This is a too large a difference to attribute to limitations in the calculation. Notice that, for the  $[\text{Co(III)}(\text{NH}_3)_5(\text{CO}_3)]^+$  complex, the difference between calculated and experimental frequencies is hardly larger than  $100\text{ cm}^{-1}$ , 3 times less than the difference discussed above. However, the differences for the highest  $A_1$  mode are much smaller, and this is the mode that one should use to compare values derived from carbonate complexes. A point that still remains to be understood is why a particular mode of carbonate, the highest  $A_1$  one, is more transferable from the complex to the surface than the other modes. Notwithstanding, a careful inspection on the normal vector shows that in the MD case this  $A_1$  mode is dominated by the motion of the  $\text{CO}_2$  moiety, which points outward the surface. On the contrary, the same  $A_1$  mode for the BD case is dominated by the motion of the CO moiety. Notice that, in both cases, the highest  $A_1$  mode corresponds to atomic displacements in the direction opposite to the bond.

Obviously, this explanation holds for both surface and complex carbonate species.

Now, we can turn our attention to the “in situ” experiments carried out by Iwasita et al.<sup>12</sup> who have studied the adsorption of carbonate on Pt(111) and Pt(110) single-crystal electrodes. These authors have used a Pt(111) single-crystal electrode and have measured the IR vibrations when the potential is stepped from 0.1 to 0.8 V. These authors find three features at 1328, 1455, and  $1537\text{ cm}^{-1}$  that are likely to be assigned to adsorbed carbonate species, although the authors conclude that the band at  $1330\text{ cm}^{-1}$  does not belong to the adsorbed carbonate. In monodentate complexes, a band at about  $1480\text{ cm}^{-1}$  has been observed and it has been attributed to the asymmetric (COO) vibrations involving the noncoordinated oxygen atoms.<sup>14</sup> Hence, this band is of  $B_2$  symmetry, and from the previous discussion, it cannot be used to compare surface and complex vibrations. In addition, we must stress the fact that the present calculations for the monodentate complex suggest that this band is not directly related to displacements of the carbonate nuclei. In any case, Iwasita et al.<sup>12</sup> conclude that the band near  $1455\text{ cm}^{-1}$  is due to vibrations involving the noncoordinated oxygen atoms in a MD mode.<sup>61</sup> The present theoretical results cast reasonable doubt on this assignment and would suggest that it is more likely due to a BD adsorbed carbonate. Iwasita et al.<sup>12</sup> also point out that changing the sample potential modifies the water structure at the interface and this changes the frequency of this vibrational mode. Above 0.7 V, both the  $1410\text{--}1460$  and  $1530\text{ cm}^{-1}$  features are attributed to 2-fold coordinated adsorbates. This assignment is supported by the present calculations, as the two features are close to the calculated values for the sh-BD and lg-BD within the error limits of the present calculations. We must stress the fact that the sh-BD is just the predicted stablest species. Likewise, the difference between the calculated vibrational frequency for the highest  $A_1$  normal modes for sh-BD and lg-BD is 61 or  $112\text{ cm}^{-1}$ , depending on the clusters used. The difference between the experimental bands is  $1537 - 1455 = 82\text{ cm}^{-1}$ , well within the previous values for the sh-BD to lg-BD differences. The present results strongly suggest that the species responsible for the spectra recorded by Iwasita et al.<sup>12</sup> are precisely the sh-BD and lg-BD, whereas the existence of a MD species is very doubtful. We must add that the calculated relative intensities do also agree with the present assignment; the intensity for the highest  $A_1$  normal mode for the sh-BD is significantly larger than the one for the lg-BD case. The two experimental bands at 1647 and  $1537\text{ cm}^{-1}$  do also exhibit different intensities, and the ratio is qualitatively comparable to the theoretical value.

Finally, we must caution that the values reported by Iwasita et al.<sup>12</sup> have been measured in an electrochemical environment while the present ones correspond to a gas-phase carbonate interacting with a model of Pt(111). Hence, there is not a one-to-one correspondence between the experimental system and the theoretical model. However, we have given significant arguments that the use of the present model calculations provides a reference that is more adequate than that based on carbonate complexes. However, up to this point, electric field and solvent effects have not been included, and one may wonder whether these effects would significantly modify the conclusions derived from the above discussion. Now we will present evidence that even if these effects can shift the calculated frequencies the effect is not large enough so as to change the strong conclusions reached in this work. The infrared and Raman spectra of carbonate in solutions have been reported by Oliver and Davis.<sup>62</sup> These authors found that the modes for free carbonate are hardly



changed by solvation. The only noticeable effect is a moderate splitting of the degenerate  $V_3$  mode, which leads to two peaks at 1376 and 1438  $\text{cm}^{-1}$  compared to the 1415  $\text{cm}^{-1}$  value for the free carbonate. For the remaining vibrational frequencies, the values in solution are 684, 880, and 1065  $\text{cm}^{-1}$  compared to 680, 879, and 1063  $\text{cm}^{-1}$  for the free carbonate. Thus, it cannot be claimed that solvent effects will change the present conclusions. Finally, we briefly discuss the influence of external electric fields on the vibrational spectra of adsorbed carbonate; a complete study is currently being carried out in our research group and will be reported in the near future.<sup>63</sup> For the sh-BD in the presence of a uniform electric field of  $\pm 0.01$  au, which is a typical value for electrochemical environments,<sup>48,49</sup> we found that the geometry of the adsorbed carbonate is almost unchanged, the distance to the surface is altered by less than 0.05 Å, and the carbonate geometry is hardly affected. This is very strong evidence for the existence of a covalent interaction since an ionic bond will largely respond to the external field.<sup>64–67</sup> For the  $A_1$  and  $B_2$  modes, which arise from the splitting of the degenerate mode of free carbonate, the frequency shifts by roughly  $\pm 85$   $\text{cm}^{-1}$ , depending on the orientation of the field, whereas the  $B_2$  mode appears in the 1180–1222  $\text{cm}^{-1}$  interval. These electric field effects in the vibrational frequencies are noticeable and merit further discussion<sup>49</sup> but are too small to invalidate the conclusions reached in the present study.

## VII. Conclusions

The interaction of carbon trioxide and carbonate on Pt(111) has been studied through the ab initio cluster model approach. Large cluster models have been used to simulate different active sites of the surface, and different coordination modes have been explored. The geometry optimization of the adsorbed species has been carried out using the HF wave function based method and the B3LYP hybrid DFT approach. For both approaches, the equilibrium geometry of adsorbed  $\text{CO}_3$  and  $\text{CO}_3^{2-}$  have been found to be very similar suggesting that once on the surface both molecules lead to the same adsorbed species. This is in complete agreement with previous theoretical works for oxide anions on metal surfaces.<sup>47,48</sup> According to the qualitative Mulliken population analysis, the net charge on the final species is of about  $-1.0$  e. We must stress the fact that the adsorbed species is not fully reduced suggesting the formation of a strong covalent bond; the analysis of the adsorption energies and of the changes induced by a uniform external electric field confirms that this is indeed the case. However, despite the similarity between the geometry and electronic structure of the final adsorbed species, the adsorption energies referred to  $\text{CO}_3$  and  $\text{CO}_3^{2-}$  are very different. This has been interpreted in terms of a cost–benefit analysis; adsorption of  $\text{CO}_3$  needs to overcome the surface work function to lead to adsorbed  $\text{CO}_3^-$ , whereas a net energy gain is obtained when  $\text{CO}_3^{2-}$  is adsorbed, resulting also in adsorbed  $\text{CO}_3^-$ .

The analysis of the vibrational frequencies leads to several important conclusions. The first important conclusion is that the vibrational frequencies of the adsorbed carbonate permit a clear distinction between monodentate and bidentate modes excluding the chelating coordination mode, which has vibrational frequencies similar to those of the monodentate case but with the reversal symmetry order. It is important to remark that the calculated vibrational frequencies for the adsorbed species are almost independent of the cluster size; this is in line with previous theoretical investigations in several systems.<sup>20–27</sup> The second conclusion is that vibrational frequencies of the adsorbed species are not always comparable to those of carbonate

complexes. However, it is shown that the vibrational frequency for the highest  $A_1$  normal internal mode is transferable from the complex to the surface. The analysis of the normal coordinate reveals that the reason for such behavior is simply due to the fact that the atomic displacements involved in this mode correspond to the atoms that in either case are farthest from the bonding region to the surface or to the complex metal center. Finally, we must stress that the splitting of the carbonate degenerate mode found for the monodentate adsorbed species is smaller than the one found for the bidentate mode. Indeed, this is independent of the cluster models used to simulate the Pt(111) surface. This splitting is qualitatively different than that corresponding to the carbonate complex.

Finally, we used the present theoretical information to interpret the results reported by Iwasita et al.<sup>12</sup> for adsorbed carbonate in an electrochemical environment. The present calculations suggest that the 1455  $\text{cm}^{-1}$  band recorded below 0.7 V is not due to a monodentate species but to a bidentate one. On the other hand, the assignment of the two experimental bands above 0.7 V to bidentate species is in agreement with the present theoretical values. Iwasita et al.<sup>12</sup> state that from their experimental study it is not possible to distinguish among chelating and bridging coordination modes. The present results suggest that the presence of chelating species is not responsible for the observed spectra.

In summary, the cluster model study of the interaction of  $\text{CO}_3$  and  $\text{CO}_3^{2-}$  on Pt(111) surface models has answered several open questions concerning adsorbed structure and bonding on this complicated system. It provides a reference to properly interpret the vibrational spectra of these adsorbed species. This reference is closer to the experimental situation and appears to be more adequate than the one based on the comparison to existing carbonate complexes. Even more important is the fact that the present theoretical study permits an understanding of the origin of the failure of the assignment of vibrational frequencies based on comparison to complexes.

**Acknowledgment.** The authors are indebted to Prof. Antonio Rodes for his constant open attitude to clarify many experimental details and to discuss the consequences of the calculated results in the interpretation of the experimental work in ref 12. Financial support was provided by the Spanish “Ministerio de Educación y Cultura”, Projects CICyT PB95-0847-CO2-01 and -02. The authors thank the Fundació Catalana de la Recerca and C<sup>4</sup> CESCA/CEPBA for continuously supporting the present calculations. A.M. thanks the Training and Mobility of Researchers program of the European Committee under Contract ERB FMGE CT95 0062 for making possible his sojourns in Barcelona and Tarragona. M.G.H. is grateful to the “Generalitat de Catalunya” for a predoctoral fellowship.

## References and Notes

- (1) Bockris, J. O'M.; Reddy, A. K. N. *Modern Electrochemistry*; Rosetta, A., Ed.; Plenum Press: New York, 1980.
- (2) See, for example, the special issue “Double Layer Modeling”: *Electrochim. Acta* **1996**, *41*, 1.
- (3) Clavilier, J.; Faure, R.; Guinet, G.; Durand, R. *J. Electroanal. Chem.* **1980**, *107*, 205.
- (4) Clavilier, J. *J. Electroanal. Chem.* **1980**, *107*, 211.
- (5) Ashley, K.; Pons, S. *Chem. Rev.* **1988**, *88*, 673.
- (6) Schindler, K.-M.; Hofmann, Ph.; Weiß, K. U.; Dippel, R.; Gardner, P.; Fritzche, V.; Bradshaw, A. M.; Woodruff, D. P.; Davila, M. E.; Asensio, M. C.; Conesa, J. C.; Gonzalez-Elipe, A. R. *J. Electron. Spectrosc. Relat. Phenom.* **1993**, *64/65*, 75.
- (7) Davila, M. E.; Asensio, M. C.; Woodruff, D. P.; Schindler, K.M.; Hofmann, Ph.; Weiss, K. U.; Dippel, R.; Gardner, P.; Fritzche, V.; Bradshaw, A. M.; Conesa, J. C.; González-Elipe, A. R. *Surf. Sci.* **1994**, *311*, 337.

- (8) Faguy, P. W.; Markovic, N.; Adzic, R. R.; Fierro, C. A.; Yeager, E. B. *J. Electroanal. Chem.* **1990**, 2289, 245.
- (9) Nart, F. C.; Iwasita, T. *J. Electroanal. Chem.* **1992**, 322, 289.
- (10) Nart, F. C.; Iwasita, T.; Weber, M. *Electrochim. Acta* **1994**, 39, 961.
- (11) Nart, F. C.; Iwasita, T.; Weber, M. *Electrochim. Acta* **1994**, 39, 2093.
- (12) Iwasita, T.; Rodas, A.; Pastor, E. *J. Electroanal. Chem.* **1995**, 383, 181.
- (13) Little, L. H.; Amberg, C. H. *Can. J. Chem.* **1962**, 40, 1997.
- (14) Little, L. H. *Infrared Spectra of Adsorbed Species*; Academic Press: London, 1986.
- (15) Goldsmith, J. A.; Ross, S. D. *Spectrochim. Acta* **1968**, 24A, 993.
- (16) Iwasita, T.; Rodas, A.; Pastor, E. *J. Electroanal. Chem.* **1995**, 383, 181.
- (17) Rodas, A.; Pastor, E.; Iwasita, T. *J. Electroanal. Chem.* **1994**, 369, 183.
- (18) Rodas, A.; Pastor, E.; Iwasita, T. *J. Electroanal. Chem.* **1994**, 373, 171.
- (19) Rodas, A.; Pastor, E.; Iwasita, T. *J. Electroanal. Chem.* **1994**, 377, 215.
- (20) Bagus, P. S.; Pacchioni, G.; Nelin, C. J. In *Studies in Physical and Theoretical Chemistry*; Carbo, R., Ed.; Elsevier: Amsterdam, 1989; Vol. 62, p 475.
- (21) Sauer, J. *Chem. Rev.* **1989**, 89, 199.
- (22) Ruetter, F., Ed. *Quantum Chemistry Approaches to Chemisorption and Heterogeneous Catalysis*; Kluwer Academic Publishers: The Netherlands, 1992; Vol. 6.
- (23) Whitten, J. L.; Yang, H. *Surf. Sci. Rep.* **1996**, 24, 59.
- (24) Pacchioni, G. *Heterogeneous Chem. Rev.* **1996**, 2, 213.
- (25) Wahlgren, U.; Siegbahn, P. In *Metal Ligand Interactions: From Atoms, to Clusters, to Surfaces*; Salahub, D., Russo, N., Eds.; NATO ASI Series C378; Kluwer: Dordrecht, 1991; p 199.
- (26) Illas, F.; Rubio, J.; Ricart, J. M. *J. Mol. Struct. (THEOCHEM)* **1993**, 287, 167.
- (27) Ricart, J. M.; Clotet, A.; Illas, F.; Rubio, J. *J. Chem. Phys.* **1994**, 100, 1988.
- (28) Paredes, P.; Patrito, E. M. Poster communication presented at the Surface Electrochemistry meeting held in Alicante, 1997, September 7–10 and private communication.
- (29) Sellers, H.; Patrito, E. M.; Olivera, P. P. *Surf. Sci.* **1996**, 356, 222.
- (30) Patrito, E. M.; Sellers, H.; Olivera, P. P. *Surf. Sci.* **1997**, 380, 264.
- (31) Bauschlicher, C. W., Jr. *Chem. Phys. Lett.* **1995**, 246, 40.
- (32) Becke, A. D. *J. Chem. Phys.* **1993**, 98, 5648. See also: Stephens, P. J.; Deulin, F. J.; Chabalowski, C. F.; Frisch, M. J. *J. Phys. Chem.* **1994**, 99, 11623.
- (33) Ricca, A.; Bauschlicher, C. W. *J. Phys. Chem.* **1994**, 98, 12899.
- (34) Russo, T. V.; Martin, R. L.; Hay, P. J. *J. Chem. Phys.* **1995**, 102, 8023.
- (35) Siegbahn, P. E. M.; Crabtree, R. H. *J. Am. Chem. Soc.* **1997**, 119, 3103.
- (36) Illas, F.; Mele, F.; Curulla, D.; Clotet, A.; Ricart, J. M. *Electrochim. Acta*, in press.
- (37) Lopez, N.; Illas, F. *J. Phys. Chem. B* **1998**, 102, 1430.
- (38) Illas, F.; Martin, R. L. *J. Chem. Phys.* **1998**, 108, 2519.
- (39) Caballol, R.; Castell, O.; Illas, F.; Malrieu, J. P.; Moreira, I. P. R. *J. Phys. Chem.* **1997**, 42, 7860.
- (40) Hay, P. J.; Wadt, W. R. *J. Chem. Phys.* **1985**, 82, 299.
- (41) Zurita, S.; Rubio, J.; Illas, F.; Barthelat, J. C. *J. Chem. Phys.* **1996**, 104, 8500.
- (42) Rubio, J.; Zurita, S.; Barthelat, J. C.; Illas, F. *Chem. Phys. Lett.* **1994**, 217, 283.
- (43) Zurita, S.; Rubio, J.; Illas, F. *Electrochim. Acta* **1996**, 41, 2275.
- (44) Illas, F.; Márquez, A.; Zurita, S.; Rubio, J. *Phys. Rev. B* **1995**, 52, 12372.
- (45) Illas, F.; Zurita, S.; Márquez, A.; Rubio, J. *Surf. Sci.* **1997**, 376, 279.
- (46) Illas, F.; Clotet, A.; Ricart, J. M. *J. Phys. Chem.* **1997**, 101, 9732.
- (47) Durand, P.; Barthelat, J. C. *Theor. Chim. Acta* **1975**, 38, 283.
- (48) Bagus, P. S.; Nelin, C. J.; Müller, W.; Philpot, M. R.; Seki, H. *Phys. Rev. Lett.* **1997**, 58, 559.
- (49) Bagus, P. S.; Nelin, C. J.; Hermann, K.; Philpot, M. R. *Phys. Rev. B* **1987**, 36, 8169.
- (50) Frisch, M. J.; Trucks, G. W.; Schlegel, H. B.; Gill, P. M. W.; Johnson, B. G.; Robb, M. A.; Cheeseman, J. R.; Keith, T.; Petersson, G. A.; Montgomery, J. A.; Raghavachari, K.; Al-Laham, M. A.; Zakrzewski, V. G.; Ortiz, J. V.; Foresman, J. B.; Peng, C. Y.; Ayala, P. Y.; Chen, W.; Wong, M. W.; Andres, J. L.; Replogle, E. S.; Gomperts, R.; Martin, R. L.; Fox, D. J.; Binkley, J. S.; Defrees, D. J.; Baker, J.; Stewart, J. P.; Head-Gordon, M.; Gonzalez, C.; Pople, J. A. *Gaussian 94*, revision D.2; Gaussian, Inc.: Pittsburgh, PA, 1995.
- (51) Bagus, P. S.; Illas, F.; Sousa, C.; Pacchioni, G. *Electronic properties of solids using cluster models*; Kaplan, T. A., Mahanti, S. D., Eds.; Plenum: New York, 1995.
- (52) Pacchioni, G.; Bagus, P. S. *Surf. Sci.* **1993**, 286, 317.
- (53) Bagus, P. S.; Pacchioni, G. *J. Chem. Phys.* **1995**, 102, 879.
- (54) Herzberg, G. *Infrared and Raman Spectra of Polyatomic Molecules*; Van Nostran: New York, 1945.
- (55) Nakamoto, K.; Fujita, J.; Tanaka, S.; Kobayashi, M. *J. Am. Chem. Soc.* **1957**, 79, 4904.
- (56) Fujita, J.; Martell, A. E.; Nakamoto, K. *J. Chem. Phys.* **1962**, 36, 339.
- (57) Gatehouse, B. M.; Livingstone, S. E.; Nyholm, R. S. *J. Chem. Soc.* **1958**, 3137.
- (58) Curtiss, L. A.; Raghavachari, K.; Redfern, P. C.; Pople, J. A. *J. Chem. Phys.* **1997**, 106, 1063.
- (59) Curtiss, L. A.; Raghavachari, K.; Redfern, P. C.; Pople, J. A. *Chem. Phys. Lett.* **1997**, 270, 4199.
- (60) Markovits, A.; Garcia-Hernandez, M.; Clotet, A.; Ricart, J. M.; Illas, F. To be published.
- (61) We must quote the fact that Iwasita et al., ref 12, attributed the band appearing at 1455 cm<sup>-1</sup> to a symmetric stretching; this is clearly a printing mistake since this feature corresponds to the B<sub>2</sub> mode of the monodentate carbonato complex.
- (62) Oliver, B. G.; Davis, A. R. *Can. J. Chem.* **1973**, 51, 698.
- (63) Markovits, A.; Clotet, A.; Ricart, J. M.; Garcia-Hernandez, M.; Illas, F. Work in progress.
- (64) Bagus, P. S.; Pacchioni, G.; Philpott, M. *J. Chem. Phys.* **1989**, 90, 4287.
- (65) Bagus, P. S.; Pacchioni, G. *Surf. Sci.* **1993**, 286, 317.
- (66) Ricart, J. M.; Clotet, A.; Illas, F.; Rubio, J. *J. Chem. Phys.* **1994**, 100, 1988.
- (67) Rubio, J.; Ricart, J. M.; Casanovas, J.; Blanco, M.; Illas, F. *J. Electroanal. Chem.* **1993**, 359, 167.